Relationship between ionospheric conductivity and intensity of the daytime region 1 field-aligned current in geomagnetically quiet conditions

T. Yamamoto
Department of Earth and Planetary Science, University of Tokyo, Tokyo, Japan

M. Ozaki
Institute of Industrial Science, University of Tokyo, Tokyo, Japan

S. Inoue
Faculty of Education, Iwate University, Morioka, Japan

Received 24 July 2002; revised 10 January 2003; accepted 20 February 2003; published 16 May 2003.

[1] The relationship between the region 1 field-aligned current (FAC) intensity and the ionospheric conductivity in geomagnetically quiet conditions has been believed to be useful to determine whether the FAC is driven by a voltage generator or a current generator. This paper, however, shows that at least for daytime (0800–1600 MLT) FACs, the current generator has the same characteristic of "linear relationship between the current intensity and the conductivity" as the voltage generator. This conclusion is obtained due to the fact that the sum of Pedersen conductivities, maintained by solar EUV ionization, at two conjugate points on the northern and southern ionospheres is approximately independent of the solar zenith angle at either of these points. Notably, the pressure-gradient-driven model for the generation of the region 1 FAC from the low-latitude boundary layer is then consistent with observations that the current intensity increases linearly with the height-integrated Pedersen conductivity. *INDEX TERMS:* 2736 Magnetospheric Physics: Magnetosphere/ionosphere interactions; 2731 Magnetospheric Physics: Magnetosphere—outer; 2708 Magnetospheric Physics: Current systems (2409); 2712 Magnetospheric Physics: Electric fields (2411); *KEYWORDS:* region 1 field-aligned current, ionospheric conductivity, current generator, voltage generator, low-latitude boundary layer

Citation: Yamamoto, T., M. Ozaki, and S. Inoue, Relationship between ionospheric conductivity and intensity of the daytime region 1 field-aligned current in geomagnetically quiet conditions, *J. Geophys. Res.*, *108*(A5), 1190, doi:10.1029/2002JA009607, 2003.

1. Introduction

[2] The characteristics of generation mechanisms of large-scale field-aligned currents (FACs) have been discussed in view of the relative importance of a voltage generator and a current generator, by several authors [*Fujii et al.*, 1981; *Robinson*, 1984; *Lysak*, 1985; *Vickrey et al.*, 1986; *Fedder and Lyon*, 1987; *Fujii and Iijima*, 1987; *Siscoe et al.*, 1991; *Siscoe and Maynard*, 1991]. *Fedder and Lyon* [1987] performed an MHD simulation for the solar wind-magnetosphere-ionosphere coupling in conditions of strongly southward IMF (interplanetary magnetic field). The dynamo in their model does not appear to be either of a pure voltage generator or a pure current generator: as the ionospheric conductivity increases, the total cross polar cap potential decreases and the total current in the region 1 FAC system increases. The dynamo is located on open field lines, and the driven region 1 currents are centered on the last closed field lines; this point is not consistent with some observations that intense region 1 FACs flow near the inner (equatorward) edge of the population of particles precipitating from the low-latitude boundary layer (LLBL) (see the introduction by *Yamamoto et al.* [2002]).

[3] *Siscoe et al.* [1991] proposed a model of the convection current system with a voltage generator in the HLBL (high-latitude boundary layer) and a current generator in the LLBL: FACs result from viscous solar wind coupling while the voltage generator results from a fraction of the solar wind motional electric field penetrating the HLBL. The viscous interaction model, however, does not conform with the observation of hourly values of the solar wind speed and the densities of region 1 FACs in the daytime (0800–1600 MLT) sectors, which shows a poor correlation between these two quantities [*Iijima and Potemra*, 1982]. As an extension of the model by Siscoe et al., *Siscoe and Maynard* [1991] numerically obtained a two-dimensional pattern of the region 1 and region 2 FACs characterized by two sets of nested spirals. However, the spirals structured such that the latitudinal width of each current layer systematically varies with MLT could not be

0148-0227/03/2002JA009607

identified in either of the statistical [e.g., *Iijima and Potemra*, 1978] and instantaneous [e.g., *Richmond et al.*, 1988] plots of observed FACs.

[4] Recently, *Yamamoto et al.* [2002] showed that region 1 FACs are inevitably produced in the LLBL region by a pressure-gradient-driven mechanism, whenever magnetosheath particles enter that region. The ultimate cause of the FAC generation is nonalignment of the LLBL inner edge with the average magnetic drift direction. This mechanism is categorized as a current generator because the sum of region 1 current intensities on both hemispheres is assumed to be insensitive to the dipole tilt angle (namely, it is insensitive to the ionospheric conductivity in quiet conditions). The current density/intensity distributions numerically evaluated for a plausible profile of the LLBL particle population in the framework of the *Tsyganenko* [1989] model are consistent with observations. Particularly, the pressure-gradient-driven mechanism is supported by the observations by the Viking satellite, i.e., the (above-mentioned) colocation of intense region 1 FACs and the inner edge of the region of precipitating LLBL particles [*Potemra et al.*, 1987; *Bythrow et al.*, 1987] and the positive correlation between the region 1 FAC intensity and the LLBL ion energy density in the 0400–1030 MLT range under northward IMF conditions [*Woch et al.*, 1993].

[5] *Lysak* [1985] theoretically studied the effect of the internal conductivity (Σ_G) of an FAC generator on the characteristics of the generator, assuming that FACs are carried by shear Alfvén waves. A variety of states intermediate between the pure current ($\Sigma_G = 0$) and pure voltage (Σ_G to ∞) generators were shown to appear depending on the ratio of the generator conductivity to the ionospheric Pedersen one. (*Lysak* [1985], however, did not address any specific physical mechanism for driving FACs or Alfvén waves, i.e., the charge separation process in the magnetosphere.) In the present paper, such an intermediate property of the generator, arising from the Alfvén wave propagation, is not studied, and the (pure) voltage and current generators are then defined as follows: If the peak magnitude of the (ionospheric) electric field across the longitudinal zone of the region 1 or region 2 FAC is independent of the ionospheric conductivities, the FAC is assumed to be supplied from a voltage generator; if the total amount of FACs supplied from a generator into both hemispheres is independent of the ionospheric conductivities, it is a current generator.

[6] *Fujii et al.* [1981] examined the seasonal dependence of large-scale FACs, using the TRIAD satellite data. They found that the intensities of region 1 FACs are larger during periods of increased ionospheric conductivity and suggested that these currents are supplied from a voltage generator in the magnetosphere. *Vickrey et al.* [1986] suggested, from the HILAT satellite data of electric fields and currents, that intermediate-scale (3–80 km) FACs are controlled by a constant current generator. *Fujii and Iijima* [1987] (which is hereafter referred to as FI) investigated even more systematically the dependence of large-scale FACs on the ionospheric conductivities using the magnetic field data from the Magsat satellite in geomagnetically quiet conditions. In such conditions, variations of the ionospheric conductivities in the aurora oval except in the midnight sector were assumed to be governed by solar EUV ionization. It was shown that the region 1 current intensities are proportional linearly to the conductivities in a wide range of MLT, suggesting that the region 1 currents are primarily driven by voltage generators. The present paper, however, shows that at least for daytime (0800–1600 MLT) FACs, the current generator also has a characteristic of "linear relationship between the current intensity and the ionospheric conductivity" (just as the voltage generator) in the situation that the ionospheric conductivity is maintained by solar EUV ionization. This characteristic is deduced from the fact that the sum of Pedersen conductivities at a pair of conjugate points on the northern and southern ionospheres is approximately independent of the solar zenith angle. Since this fact seems to have been overlooked so far, the voltage generator only has been believed to have a linear relation between the current intensity and the conductivity. The main purpose of the present paper is then to reformulate the current intensity-conductivity relationship for a current generator, taking into account the constancy of the sum of conductivities at northern and southern conjugate points.

2. Characteristics of Current Generator and Voltage Generator

[7] According to FI, in such quiet conditions as auroral electrojet activity (AL) less than 50 nT and geomagnetic activity K_P less than 1°, the effect of particle precipitation on the Pedersen conductivity may be neglected at any local time except for midnight ones; *Mehta*'s [1978] empirical formula for the height-integrated Pedersen conductivity Σ_P controlled mainly by solar EUV radiation may then be adopted:

$$\Sigma_P \text{ (mho)} = 12.579 - 0.112\chi \quad \text{for} \quad 45^\circ \le \chi \le 95^\circ \tag{1}$$

$$= 1.939 \quad \text{for} \quad \chi > 95^\circ \tag{2}$$

where χ is the solar zenith angle.

[8] The relationship between the FAC intensity and the Pedersen conductivity is analytically derived in the same way as FI. Coupling between the FACs and the Pedersen currents in the ionosphere may be expressed as

$$J_{\|i} = -\Sigma_P \mathrm{div}_i \boldsymbol{E_i} \tag{3}$$

where $J_{\|i}$ is the FAC density at an altitude just above the ionosphere, $\boldsymbol{E_i}$ is the ionospheric electric field, div_i is the two-dimensional differential divergence operator on the ionospheric plane. The magnetic field is assumed to be equipotential and perpendicular to the ionospheric plane. It is also assumed that Σ_P is uniform. This is a good approximation for geomagnetically quiet periods because the conductivity is primarily determined by solar EUV ionization. Note that the divergence of the Hall current is negligible for uniform height-integrated conductivities. Assuming that the FAC flows in a longitudinally uniform and infinite current sheet, its intensity, I, is given by

$$I = -\Sigma_P (E^p - E^e) \tag{4}$$

where superscripts p and e denote the poleward and equatorward boundaries of the region 1 or region 2 FAC zone, respectively. Specifically, the magnitudes of region 1 and region 2 current intensities, I_1 and I_2, are written as

$$|I_1| \sim 2\Sigma_P|E_1^p| \sim 2\Sigma_P|E_1^e| \tag{5}$$

$$|I_2| \sim 2\Sigma_P|E_2^p| \sim 2\Sigma_P|E_2^e| \tag{6}$$

where E_1 and E_2 are electric fields arising from the region 1 and region 2 currents, respectively, and the current sheet approximation is again used. Under the assumption of equipotential field lines, the ratio between the FAC intensities, I_N (=$I_{1,N}$ or $I_{2,N}$) and I_S, at the northern and southern foot points of a given field line, respectively, is approximately equal to the ratio between $\Sigma_{P,N}$ and $\Sigma_{P,S}$ at these points:

$$I_N/I_S = \Sigma_{P,N}/\Sigma_{P,S} \tag{7}$$

[9] For the case of a voltage generator, $E^p(E^e)$ is independent of $\Sigma_{P,N}$ or $\Sigma_{P,S}$. The current intensity vs. conductivity relation is then found from equation (4):

$$I_N = K\Sigma_{P,N} \quad \text{and} \quad I_S = K\Sigma_{P,S} \tag{8}$$

where K is a constant.

[10] For the case of a current generator, $I_N + I_S$ is independent of $\Sigma_{P,N}$ or $\Sigma_{P,S}$, i.e., $I_N + I_S = C$ where C is a constant. Combination of this relation and equation (7) yields

$$\left\{\left(\Sigma_{P,N} + \Sigma_{P,S}\right)/\Sigma_{P,N}\right\}I_N = C \tag{9}$$

As will be shown in the next section, the condition of constant $\Sigma_{P,N} + \Sigma_{P,S}$ is well satisfied unless either of the two observation points conjugate with each other is located in the unilluminated area where $\chi > 95°$. In this case, equation (9) is rewritten as

$$I_N = K'\Sigma_{P,N} \quad \text{and} \quad I_S = K'\Sigma_{P,S} \tag{10}$$

where K' is a constant. Interestingly, this is the same form as in the case of a voltage generator. If the conjugate point (say, in the Southern Hemisphere) of an observation point (in the Northern Hemisphere) is located in the unilluminated area of $\chi > 95°$, the aforementioned constancy of $\Sigma_{P,N} + \Sigma_{P,S}$ does not hold true. Instead, putting $\Sigma_{P,S}$ as $\Sigma_{P,0}$, the minimum value of $\Sigma_{P,S}$, equation (9) is rewritten as

$$I_N = C\left\{\Sigma_{P,N}/\left(\Sigma_{P,N} + \Sigma_{P,0}\right)\right\} \tag{11}$$

This is the relationship which was raised by FI as a characteristic of a current generator in contrast to that of a voltage generator (see equation (4) and Figure 1a both in FI). Practically, for daytime FAC systems, equation (10) is well satisfied in a wide range of $\Sigma_{P,N(S)}$, which will be shown later by numerical calculations. It should be noted that Figure 1a of FI does not represent a general property of a current generator.

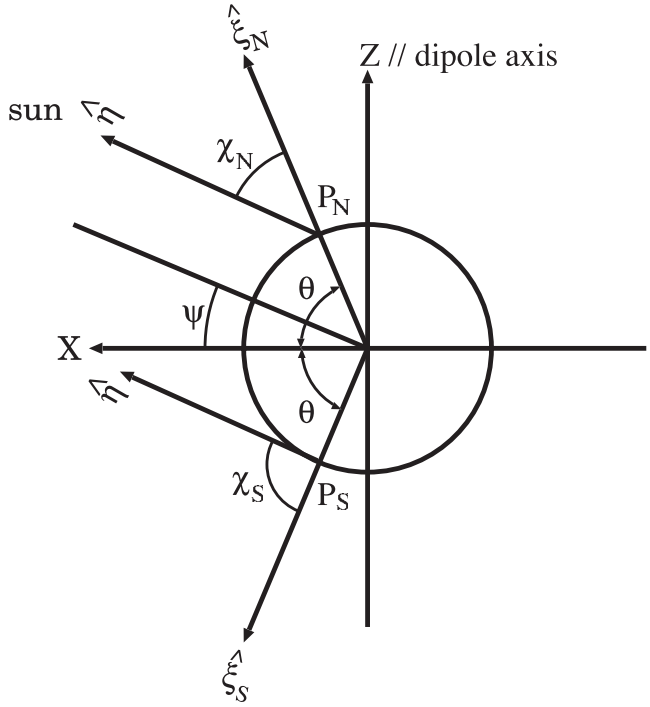

Figure 1. Schematic showing the relation between solar zenith angles χ_N and χ_S at a pair of conjugate points P_N and P_S on the northern and southern ionospheres, respectively. Points P_N and P_S are located at the noon meridian. For details, see text.

3. Constancy of $\chi_N + \chi_S$

[11] Whether or not the current generator has a characteristic of linear relationship between I_N and $\Sigma_{P,N}$ depends on the constancy of $\Sigma_{P,N} + \Sigma_{P,S}$ (see equation (9)). The sum of $\Sigma_{P,N} + \Sigma_{P,S}$ is related to that ($\chi_N + \chi_S$) of a pair of solar zenith angles at northern and southern conjugate points:

$$\Sigma_{P,N} + \Sigma_{P,S} = 12.579 \times 2 - 0.112(\chi_N + \chi_S) \tag{12}$$

for $45° \le \chi_N, \chi_S \le 95°$ (see equations (1) and (2)). The degree of constancy of $\Sigma_{P,N} + \Sigma_{P,S}$ may be measured by a relative variance of $\Sigma_{P,N} + \Sigma_{P,S}$ which is defined as

$$\delta\left(\Sigma_{P,N} + \Sigma_{P,S}\right) \equiv \frac{\left(\Sigma_{P,N} + \Sigma_{P,S}\right)_{max} - \left(\Sigma_{P,N} + \Sigma_{P,S}\right)_{min}}{\left\{\left(\Sigma_{P,N} + \Sigma_{P,S}\right)_{max} + \left(\Sigma_{P,N} + \Sigma_{P,S}\right)_{min}\right\}/2} \tag{13}$$

where $(\Sigma_{P,N} + \Sigma_{P,S})_{max}$ and $(\Sigma_{P,N} + \Sigma_{P,S})_{min}$ are maximum and minimum values of $\Sigma_{P,N} + \Sigma_{P,S}$ in the range of $45° \le \chi_N, \chi_S \le 95°$. From (12), $\delta(\Sigma_{P,N} + \Sigma_{P,S})$ is written as

$$\delta\left(\Sigma_{P,N} + \Sigma_{P,S}\right) = \frac{0.112\left\{(\chi_N + \chi_S)_{max} - (\chi_N + \chi_S)_{min}\right\}}{12.579 \times 2 - 0.112\left\{(\chi_N + \chi_S)_{max} + (\chi_N + \chi_S)_{min}\right\}/2} \tag{14}$$

This quantity will be evaluated in both cases of the pure dipole field and the 1989 Tsyganenko [*Tsyganenko*, 1989] model (which is hereafter referred to as T89), by examining the relation between χ_N and χ_S. In applying T89, a dipole field is used as the field from the Earth's interior, and only the $K_P = 0$ model is chosen because the I-Σ_P relations in the aforementioned quiet conditions are exclusively considered. The magnetic fields in the model are symmetric with respect to the noon-midnight meridional plane, i.e., they have a dawn-dusk symmetry.

[12] First, as illustrated in Figure 1, suppose a simplest case that conjugate points P_N and P_S are at the noon meridian and they are on the northern and southern ionospheres and connected by a dipole field line. Let the solar zenith angles at P_N and P_S be χ_N and χ_S, respectively. They are related to the geomagnetic latitude θ (>0) and the dipole tilt angle ψ:

$$\chi_N = \theta - \psi \tag{15}$$

$$\chi_S = \theta + \psi \tag{16}$$

Therefore $\chi_N + \chi_S$ is exactly constant, independent of ψ, i.e., $\chi_N + \chi_S = 2\theta$.

[13] Next, the solar zenith angle at any local time is considered. Suppose that P_N is located at latitude θ and longitude ϕ, where θ and ϕ are defined, in terms of the solar magnetic coordinates (X, Y, Z), as $\theta = \arctan\left(|Z|/\sqrt{X^2+Y^2}\right)$ and $\phi = \arccos\left(X/\sqrt{X^2+Y^2}\right)$, respectively. When the field lines are symmetric with respect to the X-Y plane, which is the case with the dipole field, (X, Y, Z) at P_N and P_S are expressed as

$$(X, Y, Z) = (a\cos\theta\cos\phi, a\cos\theta\sin\phi, \pm a\sin\theta) \tag{17}$$

where a is the Earth's radius, and the plus and minus signs are for P_N and P_S, respectively. The unit vectors aligned with the zenith directions at P_N and P_S are then given by

$$\hat{\boldsymbol{\xi}} = (\cos\theta\cos\phi, \cos\theta\sin\phi, \pm\sin\theta) \tag{18}$$

The unit vector, $\hat{\boldsymbol{\eta}}$, directed sunward is

$$\hat{\boldsymbol{\eta}} = (\cos\psi, 0, \sin\psi) \tag{19}$$

The solar zenith angles χ_N and χ_S are derived from the relation of $\cos\chi = \hat{\boldsymbol{\xi}} \cdot \hat{\boldsymbol{\eta}}$:

$$\cos\chi = \cos\theta\cos\phi\cos\psi \pm \sin\theta\sin\psi \tag{20}$$

The relative variance $\delta(\Sigma_{P,N} + \Sigma_{P,S})$ can now be evaluated by solving numerically the above equation (with ψ given appropriately) for χ_N and χ_S. Actually, $\delta(\Sigma_{P,N} + \Sigma_{P,S})$ in the range of $45° \le \chi_N, \chi_S \le 95°$ is calculated for θ = 60, 65, 70, 75 and 80 degrees and MLT = 0600 (or 1800) and 0900 (or 1500) hours. All the variances are found to be less than 0.01. It is then inferred that $\Sigma_{P,N} + \Sigma_{P,S}$ is nearly constant in wide ranges of the latitude and MLT, if χ_N and χ_S are in the range of $45° \le \chi \le 95°$. Note that in the nighttime (0000 < MLT < 0600 and 1800 < MLT < 2400) sectors, the Σ_P-range corresponding to $45° \le \chi_N, \chi_S \le 95°$ is so limited that the constancy of $\Sigma_{P,N} + \Sigma_{P,S}$ is unimportant for the I-Σ_P relation.

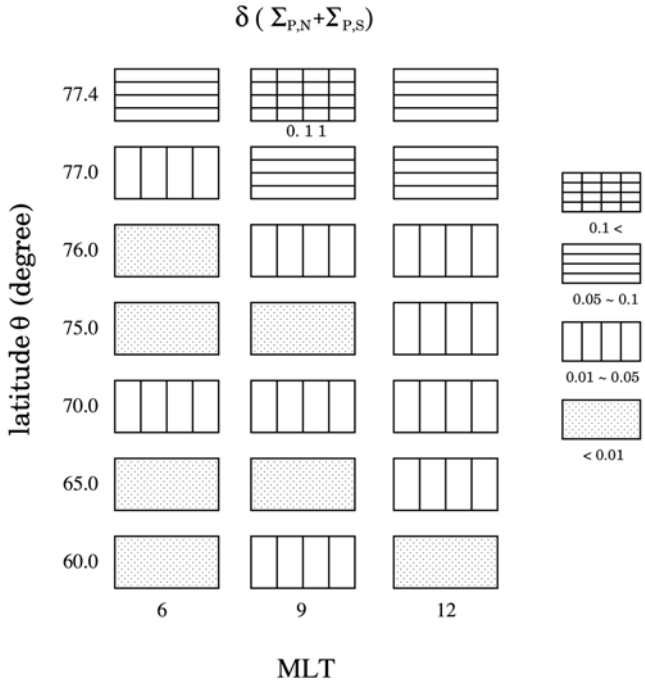

Figure 2. Relative variances of $\delta(\Sigma_{P,N} + \Sigma_{P,S})$ in the range of $45° \le \chi_N, \chi_S \le 95°$ at various latitudes and local times. Their magnitudes are indicated by different patterns in respective cells. At latitudes higher than 77.5°, at least one of the three points at 0600, 0900, and 1200 MLT has no conjugate point for certain values of the dipole tilt angle, namely the corresponding field line is not closed. The same profiles are obtained for the afternoon (MLT > 1200) side, due to the dawn-dusk symmetry of the model fields.

[14] In the present paper the nighttime sector is defined as mentioned above; the local time range of 0800 < MLT < 1600 is referred to as the daytime sector, and other ranges of 0600 < MLT < 0800 and 1600 < MLT < 1800 are the dawn and dusk sectors, respectively. As will be discussed later, the I-Σ_P relations in the daytime, dawn/dusk, and nighttime sectors are characterized by three distinct profiles (see Figures 3a, 3b, and 3c). At the same time, the domains of region 1 currents in the daytime and nighttime sectors are generally characterized by the precipitations of particles mainly from the low-latitude boundary layer and from the plasma sheet, respectively; mixed precipitations of these two species of particles are often observed in the region 1 domains in the dawn/dusk sectors [*Woch et al.*, 1993; *Newell and Meng*, 1994].

[15] For the case of T89 with $K_P = 0$, Figure 2 shows $\delta(\Sigma_{P,N} + \Sigma_{P,S})$ in the range of $45° \le \chi_N, \chi_S \le 95°$. The variances are larger than in the dipole case, but they are still sufficiently small to justify the approximation of $\Sigma_{P,N} + \Sigma_{P,S} \sim const$. Finally, note the followings: In reality, due to nonzero dipole tilt, a pair of conjugate points P_N and P_S are not symmetrically located with respect to the equatorial

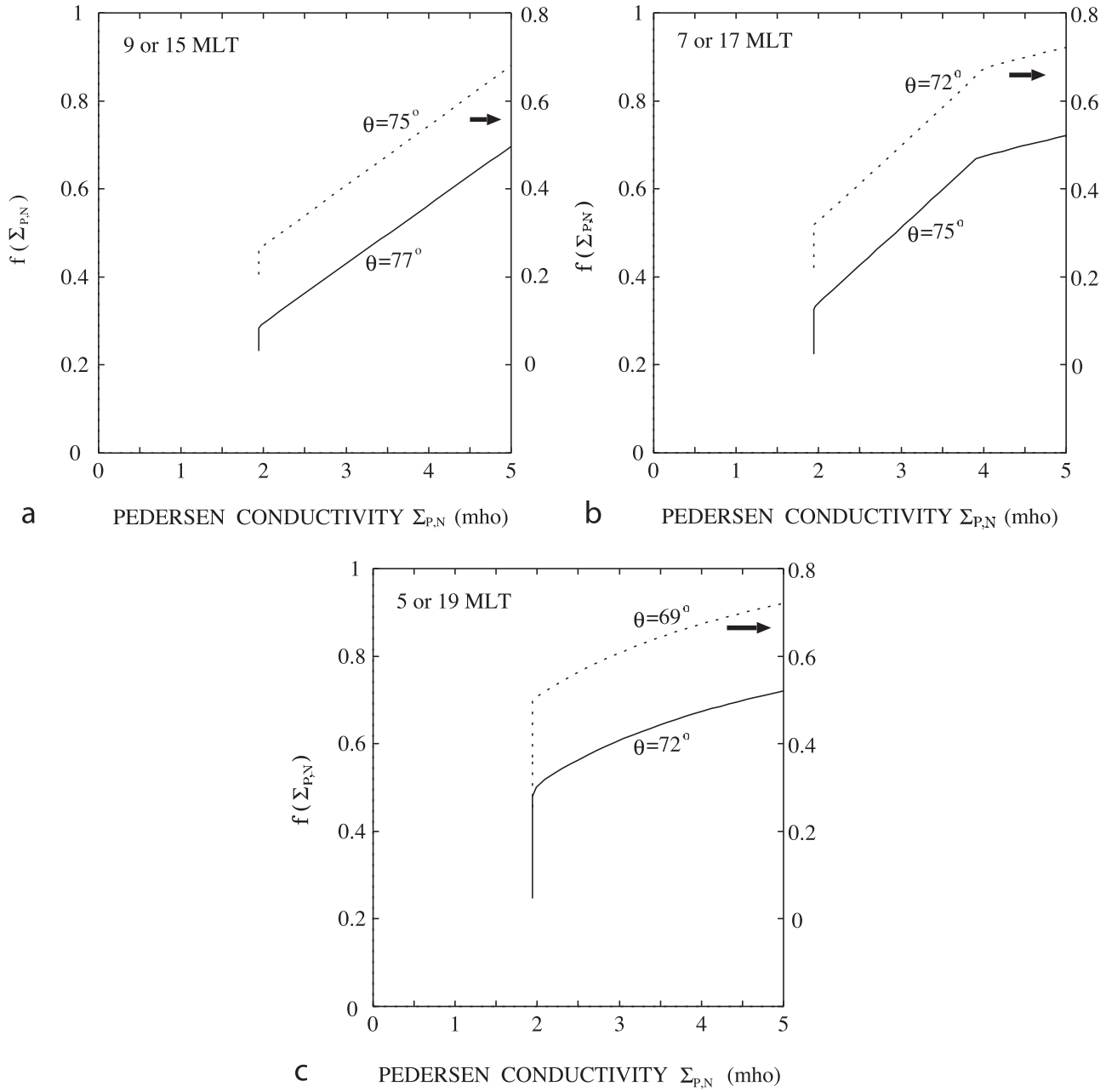

Figure 3. Functions of $f(\Sigma_{P,N})$ at various latitudes and local times of (a) 9 or 15 hours, (b) 7 or 17 hours, and (c) 5 or 19 hours. In each case, the ordinates on the left and right sides are for $f(\Sigma_{P,N})$ at high and low latitudes, respectively.

plane. This is the reason why the Tsyganenko model is used instead of the pure dipole field.

4. Relationship Between *I* and Σ_p

[16] On evaluation of $\Sigma_{P,N}$ and $\Sigma_{P,S}$ as functions of χ_N (or ψ), it is straightforward to obtain a relationship (equation (9)) between I_N and $\Sigma_{P,N}$, in the case of a current generator:

$$I_N = C\{\Sigma_{P,N}/(\Sigma_{P,N} + \Sigma_{P,S})\} \equiv Cf(\Sigma_{P,N}) \qquad (21)$$

The relation is essentially characterized by a function $f(\Sigma_{P,N})$ defined above. For the case of T89, Figures 3a 3b and 3c show $f(\Sigma_{P,N})$ at various latitudes and local times of 9 or 15 hours, 7 or 17 hours, and 5 or 19 hours, respectively. These locations are chosen so that $f(\Sigma_{P,N})$ may correspond to the scatter plots from the observations of region 1 FACs in Figure 3 of FI. Functions of $f(\Sigma_{P,N})$ are calculated for $|\psi| \leq 34°$, and displayed in the range of $\Sigma_{P,N} \leq 5$ mho, where data points are present in the scatter plots of the current intensity versus the Pedersen conductivity in FI. In Figure 3b, three parts with different slopes can be distinguished: the left one is a vertical line segment at $\Sigma_{P,N} = \Sigma_{P,0} = 1.939$ mho (corresponding to the condition of $\chi_N \geq 95°$), the middle one is almost a straight line (equation (10)) due to the constancy of $\Sigma_{P,N} + \Sigma_{P,S}$,

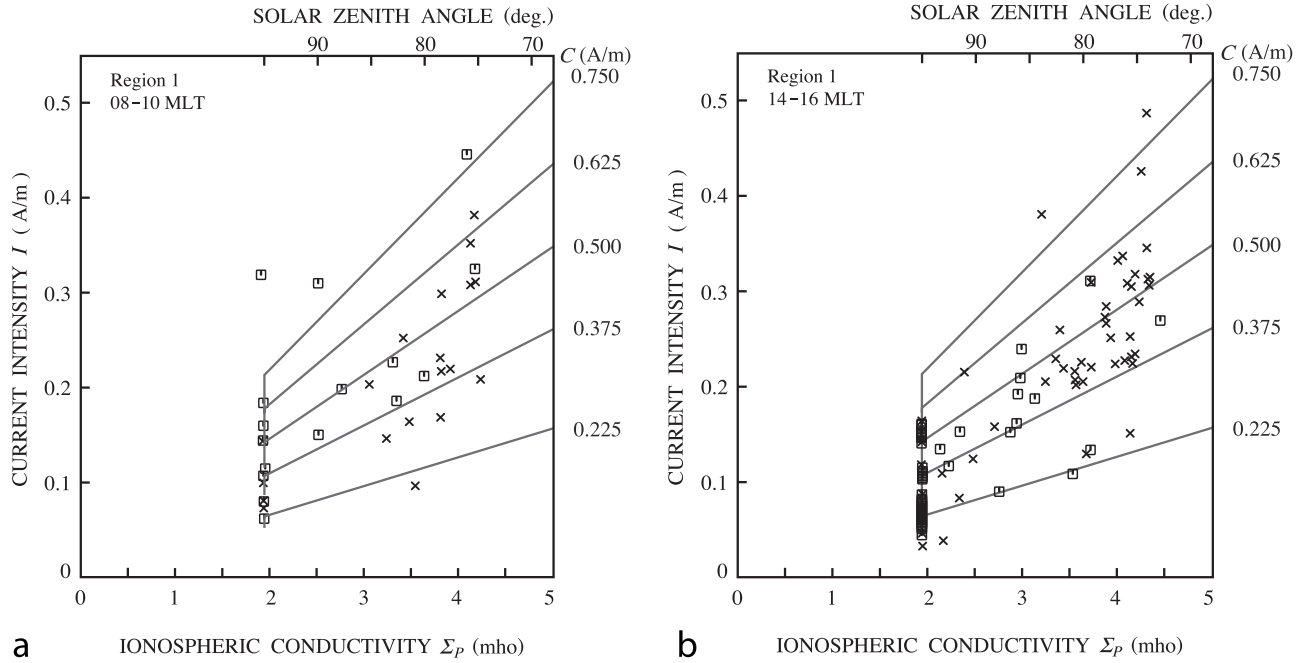

Figure 4. Theoretical relations (in red) between I and Σ_P superposed on the observed scatter plots in (a) 0800–1000 MLT and (b) 1400–1600 MLT. Assumed values of C ($\equiv I_N + I_S$) are indicated. See color version of this figure at back of this issue.

and the right one is a curved line (equation (11)). In Figure 3a the first two types of lines appear. In Figure 3c the first and third types appear. These facts can be easily understood by considering the difference in MLT: In the daytime sector (Figure 3a) the conjugate point is illuminated, i.e., $45° \leq \chi_S \leq 95°$ when χ_N is greater than about 68°, i.e., $\Sigma_{P,N} \leq 5$ mho, so that a (curved) line with a gentle slope does not appear in the range of $\Sigma_{P,N} \leq 5$ mho. In the dawn/dusk sector (Figure 3b), χ_S is greater than 95° when $\Sigma_{P,N}$ is greater than a certain value of less than 5 mho so that a line with a gentle slope appears in the range of $\Sigma_{P,N} \leq 5$ mho. In the nighttime sector (Figure 3c) the conjugate point is unilluminated, i.e., $\chi_S > 95°$ so that a straight line with $\Sigma_{P,N} + \Sigma_{P,S} \sim const$ disappears.

[17] If a constant C ($\equiv I_N + I_S$) is given, the I-Σ_P relation is determined from $f(\Sigma_{P,N})$ in Figure 3. In Figure 4, I-Σ_P relations with various values of C at $\theta = 77°$ and MLT = 0900 or 1500 are superimposed on the observed scatter plots in 0800–1000 and 1400–1600 MLT, reproductions of Figures 3c and 3d of FI. It is found that most of the data points lie in the regions swept by theoretical lines with values of C in an appropriate range. (Several outliers appear outside the domains of those theoretical lines. One possible reason for this is that a temporal fluctuation in the perturbed magnetic field happens to be identified as a signature of the spatial structure of a region 1 current.) Therefore the observed correlations between the region 1 current intensity and the Pedersen conductivity at these local times in quiet conditions may be interpreted as a manifestation of the current generator. As noted earlier, however, those observations are also consistent with the characteristic of a voltage generator. This point will be further discussed in the next section. The I-Σ_P relations for the region 1 currents at other local times as well as the region 2 current are discussed in Appendix A.

5. Concluding Remarks

[18] It has been shown that for daytime (0800–1600 MLT) region 1 FACs, a current generator has the same characteristic of linear relationship between the current intensity and the ionospheric conductivity as a voltage generator, in the situation that the ionospheric conductivity is maintained by solar EUV ionization. This means that one cannot predict, from observed correlation between the current intensity and the ionospheric conductivity in geomagnetically quiet conditions, which mechanism, a current generator or a voltage generator, actually produces the FACs. Such a prediction is possible using other observations. In fact, as for the region 1 current from the low-latitude boundary layer (LLBL), *Yamamoto et al.* [2002] have shown that the pressure-gradient-driven mechanism, i.e., the current generator is supported by various observations, such as the colocation of intense region 1 FACs and the inner edge of the region of precipitating LLBL particles and the positive correlation between the current intensity and their kinetic energy density. On the contrary, other theoretical models for the LLBL region 1 current (including a voltage generator) do not seem to be consistent with observations (see introduction).

Appendix A: I-Σ_p Relations for Region 2 and Nighttime Region 1 FACs

[19] The refractive lines for 0700 or 1700 MLT in Figure 3b appear to be inconsistent with the corresponding

observed scatter plots of I versus Σ_P for 0600 < MLT < 0800 and 1600 < MLT < 1800 (in Figure 3 of FI). This implies that the I-Σ_P relation for dawn/dusk region 1 FACs may not be understood as a characteristic of a pure current generator. Some complexity might arise from dual current sources in the plasma sheet (PS) and the low-latitude boundary layer (LLBL), particularly at these local times in quiet conditions (see, e.g., *Woch et al.* [1993]). In Figure 3c the slopes appear to be too gentle to be fitted to the corresponding scatter plots for 0400 < MLT < 0600 and 1800 < MLT < 2000. This also suggests that the generation of (nighttime) region 1 FACs originating from the PS may not simply be understood in view of the concept of a pure current generator. Even if they are produced by a pressure-gradient-driven mechanism, their development could be controlled by the convection arising from the daytime region 1 currents of LLBL origin. This is just the mechanism of convection-distortion, which was earlier proposed by *Yamamoto and Ozaki* [1993] and *Yamamoto et al.* [1996]. (In their papers, however, the solar wind convection was assumed instead of the convection attributable to the LLBL FACs; in quiet conditions the latter is considered to be a primary agent driving region 1 FACs in the PS.) In this process of convection-distortion, the electric field arising from the LLBL FACs may be termed the driving field while the one from the region 1 FACs of PS origin may be termed the reacting field. The strenghs of these fields are measured by the ratios of I/Σ_P (see equation (5)), and their typical levels are practically given by slopes of the respective regression lines representing the observed correlations between I and Σ_P (Figure 4 of FI). It is naturally expected that the reacting field is on average weaker than the driving one. This speculation is in conformity with the observations that the slopes of the regression lines for nighttime region 1 currents are smaller than those for daytime ones.

[20] A similar argument is possible about the generation of the region 2 FACs. Basically, they are assumed to be generated in the low-latitude side of the plasma sheet, by the pressure-gradient-driven mechanism. Again, they will be controlled by the development of region 1 FACs, in other words they are considered to act to shield the electrostatic fields originating from region 1 currents. This process is also categorized as the convection-distortion, and it has been numerically simulated by, e.g., *Harel et al.* [1981a, 1981b] and *Yamamoto and Inoue* [1998]. The electric field originating from the region 2 FACs is now termed the shielding field, and its typical strength is practically measured by slopes of the regression lines in Figure 6 of FI (see equation (6)). Since the shielding is generally imperfect, a typical strength of the shielding field will be weaker than that of the driving one from the region 1 FACs. This expectation is in harmony with the observations that the slopes of the regression lines for region 2 currents are significantly smaller than any one for region 1 currents.

[21] In summary, on the basis of a plausible scenario for the generations of FACs originating from the LLBL and the PS, the I-Σ_P relationship is more explicitly visualized as an idealized model. As discussed in introduction, region 1 currents will be produced in the LLBL by the pressure-gradient-driven mechanism [*Yang et al.*, 1994; *Yamamoto et al.*, 2002]. For simplicity, if the total current intensity, $I_N + I_S$, is fixed at a single value, C, the I-Σ_P relation for LLBL

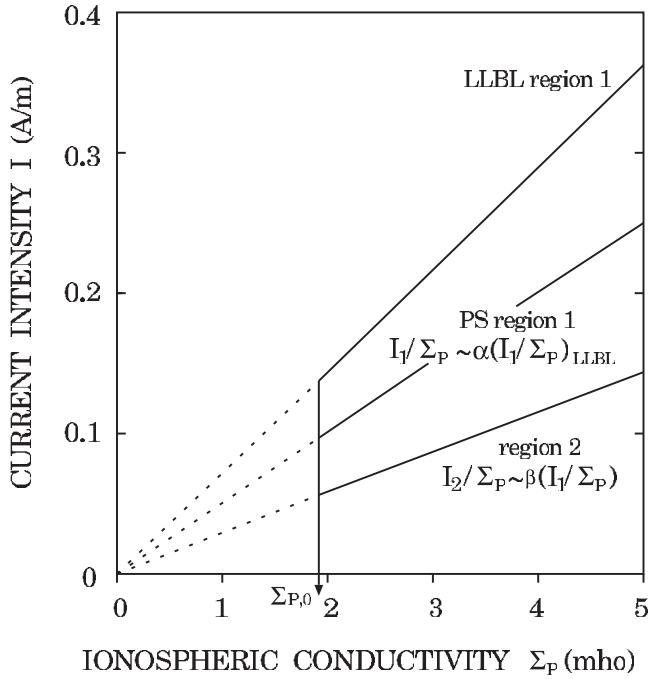

Figure 5. Prediction of the I-Σ_P relations for region 1 FACs from the LLBL and PS and a region 2 FAC. For details, see text.

FACs at, e.g., 0900 or 1500 MLT is given by a straight line passing the origin in the (I,Σ_P) coordinates because of $\Sigma_{P,N} + \Sigma_{P,S} \sim const$ in the daytime sector (see Figure 5). In reality, the straight line is meaningful for $\Sigma_P > \Sigma_{P,0}$. As mentioned above, region 1 FACs of PS origin will be produced under the influence of the convection set up by the LLBL FACs, i.e., by convection-distortion. Suppose that the strength (say, $|E_1^p|$ in equation (5)) of an electric field arising from PS region 1 FACs reach a level comparable to, but appreciably lower than that from the LLBL FACs: $|E_1^p|_{PS} \sim \alpha |E_1^p|_{LLBL}$ where $\alpha < 1$. From equation (5), $(I_1/\Sigma_P)_{PS} \sim \alpha\,(I_1/\Sigma_P)_{LLBL}$. If α is independent of Σ_P, the I-Σ_P relation for a PS region 1 current is then given by a straight line with a gentler slope, as illustrated in Figure 5. Similarly, for a region 2 FAC, its intensity I_2 will be given as βI_1, at a certain local time, where β is a measure of the efficiency of the shielding of the region 1 associated field by the region 2 one, probably significantly less than unity. Values of β have been observationally assessed in Figure 8 of FI, which are found primarily in a range of 0.3–0.8 and roughly insensitive to Σ_P and MLT. Thus the I-Σ_P relation for a region 2 current is characterized by a straight line with a slope smaller than that for a region 1 current (see Figure 5).

[22] **Acknowledgments.** The work of T. Yamamoto was supported in part by the joint research programs at the Radio Atmospheric Science Center, Kyoto University, Uji, Kyoto, and the National Institute of Polar Research, Itabashi, Tokyo.

[23] Arthur Richmond thanks Joachim Woch and another reviewer for their assistance in evaluating this paper.

References

Bythrow, P. F., T. A. Potemra, L. J. Zanetti, R. E. Erlandson, D. A. Hardy, F. J. Rich, and M. H. Acuna, High latitude currents in the 0600 to 0900 MLT sector: Observations from Viking and DMSP-F7, *Geophys. Res. Lett.*, *14*, 423–426, 1987.

Fedder, J. A., and J. G. Lyon, The solar wind-magnetosphere-ionosphere current-voltage relationship, *Geophys. Res. Lett.*, *14*, 880–883, 1987.

Fujii, R., and T. Iijima, Control of the ionospheric conductivities on large-scale Birkeland current intensities under geomagnetic quiet conditions, *J. Geophys. Res.*, *92*, 4505–4513, 1987.

Fujii, R., T. Iijima, T. A. Potemra, and M. Sugiura, Seasonal dependence of large-scale Birkeland currents, *Geophys. Res. Lett.*, *8*, 1103–1106, 1981.

Harel, M., R. A. Wolf, P. H. Reiff, R. W. Spiro, W. J. Burke, F. J Rich, and M. Smiddy, Quantitative simulation of a magnetospheric substorm: 1. Model logic and overview, *J. Geophys. Res.*, *86*, 2217–2241, 1981a.

Harel, M., R. A. Wolf, R. W. Spiro, P. H. Reiff, C.-K. Chen, W. J. Burke, F. J. Rich, and M. Smiddy, Quantitative simulation of a magnetospheric substorm: 2. Comparison with observations, *J. Geophys. Res.*, *86*, 2242–2260, 1981b.

Iijima, T., and T. A. Potemra, Large-scale characteristics of field-aligned currents associated with substorms, *J. Geophys. Res.*, *83*, 599–615, 1978.

Iijima, T., and T. A. Potemra, The relationship between interplanetary quantities and Birkeland current densities, *Geophys. Res. Lett.*, *9*, 442–445, 1982.

Lysak, R. L., Auroral electrodynamics with current and voltage generators, *J. Geophys. Res.*, *90*, 4178–4190, 1985.

Mehta, N. C., Ionospheric electrodynamics and its coupling to the magnetosphere, Ph.D. thesis, Univ. of Calif., San Diego, San Diego, Calif., 1978.

Newell, P. T., and C.-I. Meng, Ionospheric projections of magnetospheric regions under low and high solar wind pressure conditions, *J. Geophys. Res.*, *99*, 273–286, 1994.

Potemra, T. A., L. J. Zanetti, R. E. Erlandson, P. F. Bythrow, G. Gustafsson, M. H. Acuna, and R. Lundin, Observations of large-scale Birkeland currents with Viking, *Geophys. Res. Lett.*, *14*, 419–422, 1987.

Richmond, A. D., et al., Mapping electrodynamics features of the high-latitude ionosphere from localized observations: Combined incoherent-scatter radar and magnetometer measurements for January 18–19, 1984, *J. Geophys. Res.*, *93*, 5760–5776, 1988.

Robinson, R. M., Kp dependence of auroral zone field-aligned current intensity, *J. Geophys. Res.*, *89*, 1743–1748, 1984.

Siscoe, G. L., and N. C. Maynard, Distributed two-dimensional region 1 and region 2 currents: Model results and data comparisons, *J. Geophys. Res.*, *96*, 21,071–21,085, 1991.

Siscoe, G. L., W. Lotko, and B. U. Ö. Sonnerup, A high-latitude, low-latitude boundary layer model of the convection current system, *J. Geophys. Res.*, *96*, 3487–3495, 1991.

Tsyganenko, N. A., A magnetospheric magnetic field model with a warped tail current sheet, *Planet. Space Sci.*, *37*, 5–20, 1989.

Vickrey, J. F., R. C. Livingston, N. B. Walker, J. Och, T. A. Potemra, R. A. Heelis, M. C. Kelley, and F. J. Rich, On the current-voltage relationship of the magnetospheric generator at intermediate spatial scales, *Geophys. Res. Lett.*, *13*, 495–498, 1986.

Woch, J., M. Yamauchi, R. Lundin, and PotemraT. A. Zanetti, The low-latitude boundary layer at mid-altitudes: Relation to large-scale Birkeland currents, *Geophys. Res. Lett.*, *20*, 2251–2254, 1993.

Yamamoto, T., and S. Inoue, Quasi-steady production of region 1 and region 2 field-aligned currents, *Proc. NIPR Symp. Upper Atmos. Phys.*, *11*, 106–120, 1998.

Yamamoto, T., and M. Ozaki, A theory of current generator in the magnetosphere-ionosphere coupling, *Proc. NIPR Symp. Upper Atmos. Phys.*, *6*, 62–69, 1993.

Yamamoto, T., S. Inoue, N. Nishitani, M. Ozaki, and C.-I. Meng, A theory for generation of the paired region 1 and region 2 field-aligned currents, *J. Geophys. Res.*, *101*, 27,199–27,222, 1996.

Yamamoto, T., M. Ozaki, and S. Inoue, Evaluaton of the region 1 field-aligned current from the low-latitude boundary layer using the 1989 Tsyganenko model, *Adv. Polar Upper Atmos. Res.*, *16*, 13–35, 2002.

Yang, Y. S., R. W. Spiro, and R. A. Wolf, Generation of region 1 current by magnetospheric pressure gradients, *J. Geophys. Res.*, *99*, 223–234, 1994.

S. Inoue, Faculty of Education, Iwate University, Morioka, Iwate 020-8550, Japan. (inoues@iwate-u.ac.jp)

M. Ozaki, Institute of Industrial Science, University of Tokyo, Tokyo 153-850, Japan. (mozaki@iis.u-tokyo.ac.jp)

T. Yamamoto, Department of Earth and Planetary Physics, University of Tokyo, 3-1, Hongo 7 chome, Bunkyo-ku, Tokyo 113-0033, Japan. (sty@mail.ecc.u-tokyo.ac.jp)

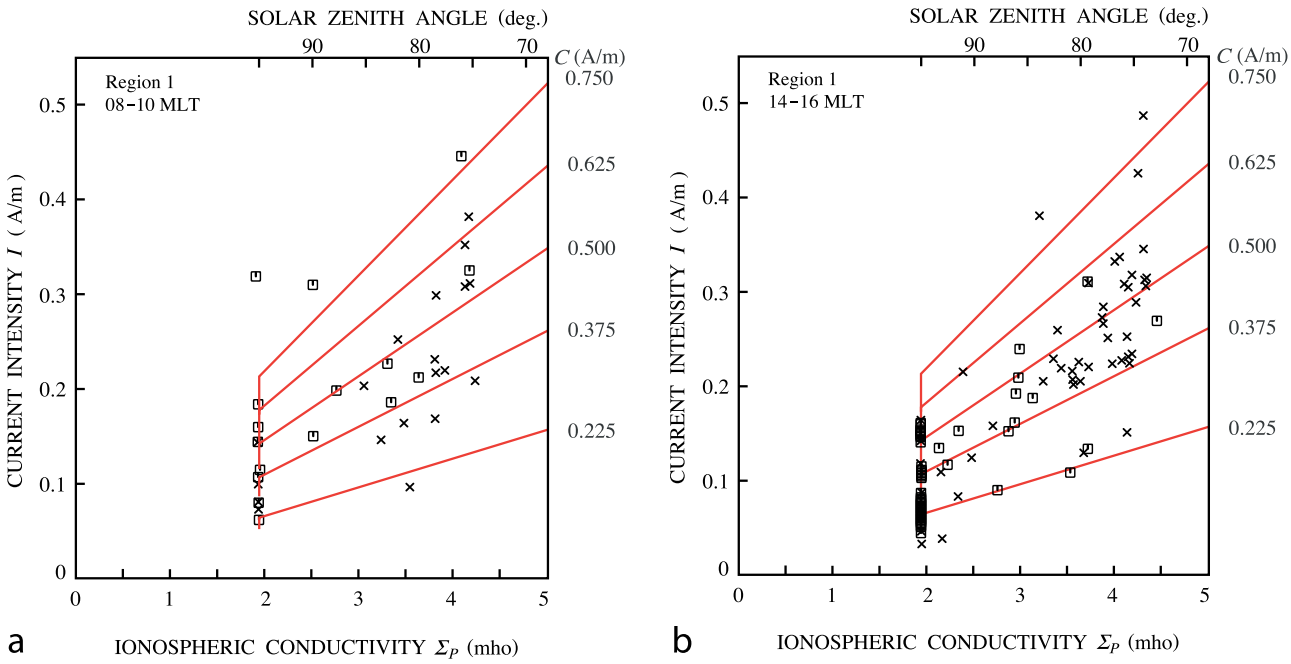

Figure 4. Theoretical relations (in red) between I and Σ_P superposed on the observed scatter plots in (a) 0800–1000 MLT and (b) 1400–1600 MLT. Assumed values of C ($\equiv I_N + I_S$) are indicated.